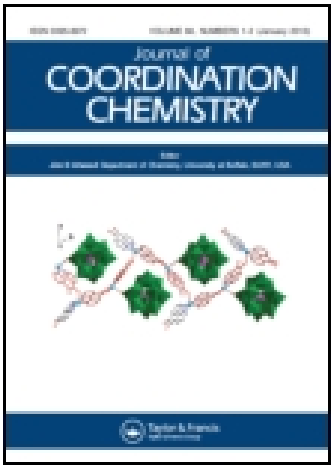

Journal of Coordination Chemistry
Publication details, including instructions for authors and subscription information:
http://www.tandfonline.com/loi/gcoo20

Hydrogen-bonded frameworks of propylenediamine-N,N′-diacetic acid Pt(II) complexes, synthesis, structural characterization, and antitumor activity

Hoda A. El-ghamry[ab], Shigeyuki Masaoka[c] & Ken Sakai[d]

[a] Faculty of Science, Chemistry Department, Tanta University, Tanta, Egypt

[b] Faculty of Applied Science, Department of Chemistry, Umm Al-Qura University, Makkah, Kingdom of Saudi Arabia

[c] Faculty of Science, Chemistry Department, Kyushu University, Fukuoka, Japan

[d] Institute for Molecular Science, Okazaki, Japan

Accepted author version posted online: 05 Mar 2014.Published online: 28 Mar 2014.

To cite this article: Hoda A. El-ghamry, Shigeyuki Masaoka & Ken Sakai (2014) Hydrogen-bonded frameworks of propylenediamine-N,N′-diacetic acid Pt(II) complexes, synthesis, structural characterization, and antitumor activity, Journal of Coordination Chemistry, 67:6, 943-955, DOI: 10.1080/00958972.2014.900550

To link to this article: http://dx.doi.org/10.1080/00958972.2014.900550

Journal of Coordination Chemistry, 2014
Vol. 67, No. 6, 943–955, http://dx.doi.org/10.1080/00958972.2014.900550

Hydrogen-bonded frameworks of propylenediamine-N, N′-diacetic acid Pt(II) complexes, synthesis, structural characterization, and antitumor activity

HODA A. EL-GHAMRY*†‡, SHIGEYUKI MASAOKA§ and KEN SAKAI¶

†Faculty of Science, Chemistry Department, Tanta University, Tanta, Egypt
‡Faculty of Applied Science, Department of Chemistry, Umm Al–Qura University, Makkah, Kingdom of Saudi Arabia
§Faculty of Science, Chemistry Department, Kyushu University, Fukuoka, Japan
¶Institute for Molecular Science, Okazaki, Japan

(*Received 24 September 2013; accepted 10 February 2014*)

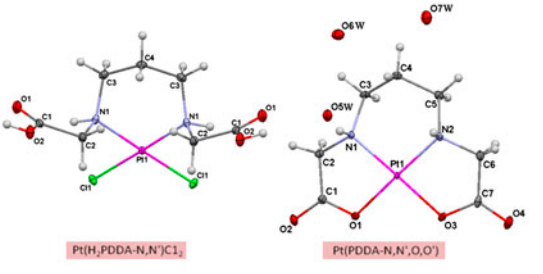

Two Pt(II) complexes of propylenediamine-N,N′-diacetic acid (H_2pdda) have been synthesized in which H_2pdda is bidentate and tetradentate. The two complexes, $[Pt(C_7H_{14}N_2O_4)Cl_2]$ (**1**) and $[Pt(C_7H_{12}N_2O_4)]$ (**2**), have been characterized by elemental analysis, IR, mass spectroscopy, and thermal (TGA and DTG) analysis. The crystal structure of **1** and $[Pt(C_7H_{12}N_2O_4)]\cdot 3H_2O$ (**2a**) are reported. *In vitro* cytotoxic properties of **1** and **2** were evaluated against HEPG2 (*liver carcinoma* cell lines) and HCT116 (*colon carcinoma* cell lines), and were compared with the standard anticancer drugs cisplatin (cis-DDP) and doxorubicin (Dox). The obtained data indicate that the two complexes show weak cytotoxic activity against the two tested cell lines, except for **1** which revealed a relatively high activity against HEPG2. Structure–activity relationships have been interpreted.

Keywords: Pt(II) complexes; H-bonded frameworks; Propylenediamine-N,N′-diacetic acid; Structural characterization; Antitumor

1. Introduction

Cis-platin (cis-diammine-dichloro-platinum(II)) was established as a drug against diverse tumor types including testicular, ovarian, head and neck, bladder, esophageal, and small cell

*Corresponding author. Email: helghamrymo@yahoo.com

lung cancer [1, 2]. However, cisplatin exhibits only limited activity against tumors like colon and breast cancer, causes considerable side effects, and induction of resistance occurs frequently [3]. Carboplatin and oxaliplatin were designed to overcome the severe side effects of cisplatin and, indeed, the replacement of the labile chlorides by a comparatively more stable bidentate O–O leaving group resulted in a modified pharmacodynamic behavior and a more tolerable toxicological profile [4, 5]. Despite the clinical success of these three compounds, their side effects [6, 7] and lack of efficacy in certain cancer types, primarily due to resistance [8], drives the search for new platinum-based anticancer agents. Leaving groups, such as chloride in cisplatin and oxalate in oxaliplatin, can modify both the kinetics of hydrolysis and the reactivity of the drug. Non-leaving groups can confer different characteristics to platinum compounds, improving their cytotoxic activity by modifying cellular uptake and the way the complex interacts with DNA [9].

Platinum(II) drugs act by direct binding to deoxyguanosine and deoxyadenosine of DNA with formation of intrastrand cross-links mainly and, to a minor degree, mono- and interstrand adducts [10]. Several platinum analogs were developed, for example, diamminecyclohexyl or ethylenediammine analogs, nedaplatin, lobaplatin, ormaplatin, iproplatin, as well as photoactivable and polynuclear complexes [11–15].

Ethylenediaminetetraacetic acid (H_4EDTA) is widely recognized as a metal complexing agent, known to bind bidentate to Pt(II) [16]. Similarly, ethylenediaminediacetic acid (H_2EDDA) is known to bind to Pt(II) bidentate, tridentate, and tetradentate [17–20]. The crystal structures of Pt(H_4EDTA-N,N′)$Cl_2\cdot 6H_2O$ [21] and Pt(H_2EDDA-N,N′)Cl_2 [22] have been previously reported. The solution behavior of Pt(EDDA-N,N′,O,O′) has been studied [20]. However, to date, there have not been reports of Pt(EDTA-N,N′,O,O′) or Pt(EDDA-N,N′,O,O′) crystal structures.

In spite of the side effects of cisplatin, the development of this compound as a successful antitumor drug is often seen as the prototypical success story. The large number of patients who have been cured after cisplatin treatment of cancer is impressive. These facts have stimulated researchers to try to mimic the structure of cisplatin but by giving specific goals. These include reduction in toxicity of cisplatin, increasing its stability and solubility in water. We describe, here, the synthesis and structure characterization of two new Pt(II) complexes of propylenediamine-N,N′-diacetic acid. The *in vitro* cytotoxic activity of the prepared complexes has been evaluated against two cell lines, HEPG2 and HCT116, with insight into the structure–activity relationship.

2. Experimental

2.1. *Materials and physical measurements*

Solvents and starting materials were purchased from TCI and Wako chemical companies, Tokyo, and used as received. Elemental analysis was carried out on a Perkin Elmer 2400II CHN. IR spectra were recorded using a Perkin-Elmer Spectrum One FT-IR spectrometer equipped with a single reflection diamond ATR accessory. ESI-TOF mass spectra (ESI-TOF MS) were recorded on a JEOL JMS-T100LC mass spectrometer. ^{1}H NMR spectra were recorded on a JEOL JNM-AL300 spectrometer using DMSO-d_6 and D_2O as solvents. Thermogravimetric analyses (TGA, DTG, and DTA) were performed on a Shimadzu TG-50 thermal analyzer in a dynamic nitrogen atmosphere with a heating rate of 10 °C min^{-1}.

2.2. *Synthesis of dichloro(propylenediamine-N,N'-diacetic acid) platinum(II) (1)*

The synthetic procedures of **1** is similar to that reported [22] for the synthesis of Pt(H_2EDDA-N,N′)Cl_2, where EDDA is ethylenediamine diacetic acid, in which 0.6 g of K_2PtCl_4 (1.445 mM) and 0.274 g of propylenediamine-N,N′-diacetic acid (1.445 mM) were dissolved in 20 mL distilled water and heated at 95 °C. After 4 h of heating, 7.5 mL of 0.1 M NaOH was added to the solution and heating was continued for an additional 3 h. At the end of the reaction, the solution becomes yellow. The resulting solution was filtered and filtrate was then evaporated to approximately 3 mL. Upon addition of 1 mL conc. HCl, light-yellow needles of the product were precipitated (scheme 1). The product was filtered off, washed with a small amount of cold water, and then dried. Yield: 0.42 g (63.9%). Anal. Calcd for [Pt($C_7H_{14}N_2O_4$)Cl_2] (**1**) (%): C, 18.43; H, 3.09; N, 6.14. Found: C, 18.37; H, 3.09; N, 6.13. TOF MS in H_2O/MeOH (–ve mode): $m/z = 455.03$. ^{1}H NMR (300 MHz, DMSO-d_6 and D_2O): $\delta = 12.27$ (2H, s, D_2O exchangeable, COOH), 6.21 (2H, s, NH) 3.84 (4H, s, CH_2COO), 2.91 (4H, t, CH_2–CH_2–CH_2), 1.94 (2H, m, CH_2–CH_2–CH_2). ^{13}C NMR (300 MHz, DMSO-d_6): δ 32.2, 44.9, 53.6, 173.2.

Faint-yellow crystals suitable for X-ray diffraction study were obtained for **1** by slow evaporation of its water solution.

2.3. *Synthesis of (propylenediamine-N,N'-diacetic acid) platinum(II) (2)*

A method similar to that of Liu [17], which was used for synthesis of Pt(EDDA-N,N′,O,O′), was used in which 0.2 g of **1** was dissolved in 10 mL of hot H_2O and treated with a hot solution of 0.136 g of Ag_2SO_4. After heating in a steam bath, the precipitated AgCl was filtered off. The filtrate was then heated with a solution of 0.138 g of $Ba(OH)_2 \cdot 8H_2O$. The precipitated $BaSO_4$ was filtered off. Evaporation of the filtrate yielded a white powder of

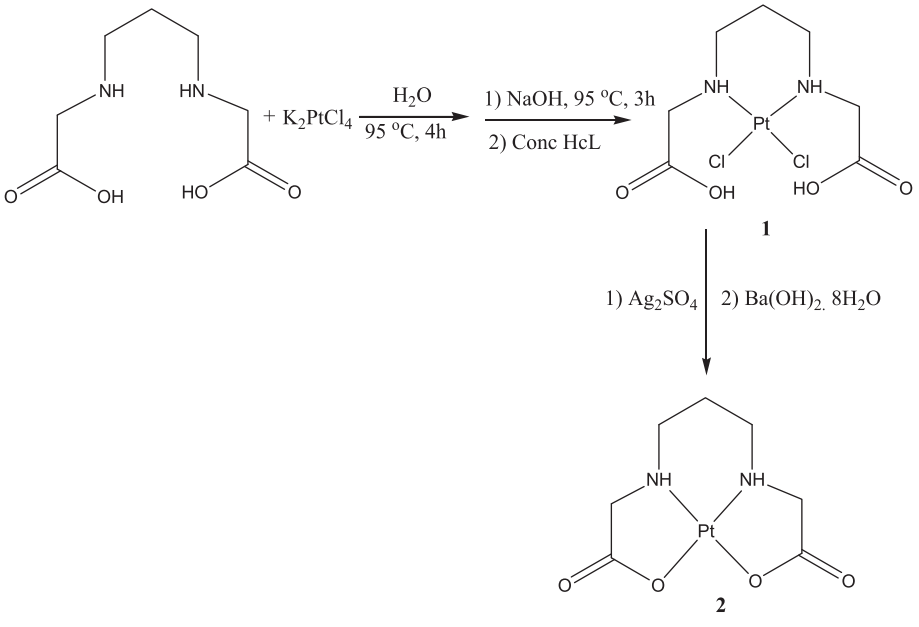

Scheme 1. Synthetic scheme for **1** and **2**.

the product which was filtered off and washed with cold water. Yield: 0.132 g (79%). Anal. Calcd for [Pt($C_7H_{12}N_2O_4$)] (**2**) (%): C, 21.94; H, 3.16; N, 7.31. Found: C, 21.03; H, 3.51; N, 7.02. TOF MS in H_2O/MeOH (–ve mode): $m/z = 383.01$. ^{1}H NMR (300 MHz, DMSO-d_6): $\delta = 6.22$ (2H, s, NH), 3.88 (4H, s, $C\underline{H_2}COO$), 2.95 (4H, t, $C\underline{H_2}$–CH_2–$C\underline{H_2}$), 1.98 (2H, m, CH_2–$C\underline{H_2}$–CH_2). ^{13}C NMR (300 MHz, DMSO-d_6): δ 32.5, 44.6, 63.1, 178.7.

Recrystallization of **2** from hot water resulted in formation of colorless crystals having the formula [Pt($C_7H_{12}N_2O_4$)]·$3H_2O$ (**2a**).

2.4. *X-ray crystallography*

Data were collected by a Bruker SMART APEX2/CCD-based diffractometer with monochromated Mo Kα radiation ($\lambda = 0.710373$ Å) from a rotating anode source with mirror-focusing apparatus. Cell parameters were retrieved using APEXII software [23] and refined using SAINT [23] on all observed reflections. Data reduction was performed using SAINT. Absorption corrections were applied using SADABS [24]. The structures were solved by direct methods using SHELXS-97 [25] and refined by least-squares on F^2 using SHELXL-97 and KENX [26] programs. The crystal data and structure refinement details of **1** and **2a** are summarized in table 1.

2.5. *Measurement of potential cytotoxicity by SRB assay*

Two human cancer cell lines were used for *in vitro* screening, *colon carcinoma* (HCT116) and *liver carcinoma* (HEPG2). They were obtained frozen in liquid nitrogen (–180 °C) from

Table 1. Crystallographic data for **1** and **2a**.

	1	**2a**
Molecular formula	$C_7H_{14}Cl_2N_2O_4Pt$	$C_7H_{18}N_2O_7Pt$
FW	456.18	437.32
Color, habit	Yellow, blocks	Colorless, blocks
Crystal size, mm	0.2 × 0.2 × 0.1	0.1 × 0.14 × 0.2
Crystal system	Orthorhombic	Monoclinic
Space group	*Pnma*	*P2(1)/c*
a, Å	10.8996(7)	9.0599(7)
b, Å	15.8790(11)	10.3613(8)
c, Å	6.6254(4)	13.3816(10)
α, °	90.00	90.00
β, °	90.00	104.4600(10)
γ, °	90.00	90.00
V, Å^3	1146.69(13)	1216.37(16)
Z	4	4
F (0 0 0)	856	808
d_{Calcd}, g/cm^3	2.654	2.355
μ(Mo Kα), mm^{-1}	12.703	11.562
T, K	100(2)	100(2)
Radiation, Å	0.71073	0.71073
Theta range, °	$2.57 < \theta < 28.74$	$2.32 < \theta < 28.26$
Index ranges	$-14 < h < 14$, $-20 < k < 20$, $-8 < l < 8$	$-12 < h < 11$, $0 < k < 13$,$0 < l < 17$
Reflections measured	12,356	2952
Unique reflections	1490	2952
Parameters refined	76	154
R(int)	0.0266	0.0000
*R*1	0.0164	0.0220
*wR*2	0.0402	0.0588
GOF	1.179	1.170
Largest diff. peak and hole (e Å^{-3})	2.112, −1.215	1.509, −2.558

the American Type Culture Collection. The tumor cell lines were maintained in the National Cancer Institute, Cairo, Egypt, by serial sub-culturing. Potential cytotoxicity of the compounds was tested using the Skehan *et al.* method [27]. Cells were plated in a 96-multiwell plate (104 cells/well) for 24 h before treatment with the compound to allow attachment of cell to the wall of the plate. Different concentrations of the compounds (0, l, 2.5, 5, l0, 15, 20, and 50 μg mL^{-1}) were added to the cell monolayer; triplicate wells were prepared for each individual dose. Monolayer cells were incubated with the compounds for 48 h at 37 °C and in atmosphere of 5% CO_2. After 48 h, cells were fixed, washed, and stained with Sulfo-Rhodamine-B stain. Excess stain was washed with acetic acid and attached stain was recovered with Tris EDTA buffer. Color intensity was measured in an ELISA reader. The relation between surviving fraction and drug cone is plotted to get the survival curve of each tumor cell line after the specified compound. Potential cytotoxicity of the compounds was measured in Pharmacology Unit, Cancer Biology Department, National Cancer Institute, Cairo University using an Elisa reader (TECAN SUNRISE). Doxorubicin (Dox) was used as a standard cytotoxin.

3. Results and discussion

3.1. *IR spectra*

The position of asymmetric stretching frequencies of carboxylate is a good tool to distinguish between the free carboxylate appearing at 1700–1750 cm^{-1} and coordinated carboxylate, which usually appears at 1600–1700 cm^{-1} [28]. Hence, in the infrared spectra of **1**, the band at 1744 cm^{-1} is assigned to the asymmetric stretch of uncoordinated carboxyl. The band corresponding to υ_{COO}(sym) appeared at 1432 cm^{-1}. In the case of **2**, the band corresponding to υ_{COO}(as) appeared at 1677 cm^{-1}. The shift of this band to lower value compared with **1** is evidence for coordination of carboxyl to Pt [28, 29]. υ_{COO}(sym) is at 1418 cm^{-1} in spectra of **2**. The band corresponding to υ_{C-O} is at 1254 and 1293 cm^{-1} in spectra of **1** and **2**, respectively, while the band corresponding to the stretching vibration of coordinated NH appeared at 3415 and 3442 cm^{-1} for **1** and **2**, respectively. Coordination of NH to Pt was confirmed by the appearance of a weak intensity band at 483 and 492 cm^{-1} in spectra of **1** and **2**, respectively, assigned to υ_{Pt-N}. In the spectrum of **2**, the band at 545 cm^{-1} was assigned to υ_{Pt-O}.

3.2. *Thermal analysis*

Thermal stability and thermal behavior of **1** and **2** were studied by thermogravimetric analysis (TG) and differential thermal gravimetry (DTG) from 25 to 800 °C. The TG and DTG curves are illustrated graphically in figures 1 and 2. Both complexes showed a two-step mass loss. Complex **1** exhibited stability to 188 °C. The fi Th mass loss of 34.92% occurred at 188–294 °C (calculated mass loss 35.29%), and corresponds to the removal of $2Cl^-$ ions and $2CO_2$ molecules from the free carboxylic acid groups. This step is accompanied by a DTG peak with maximum at 238 °C. The second step of decomposition appeared at 294–441 °C and corresponded to complete decomposition of the ligand leaving behind metallic Pt as final product. The calculated and observed mass loss within this step match each other (mass loss, calcd: 37.61%, found: 37.98%). The DTG peak maximum which is associated with this step appeared at 415 °C.

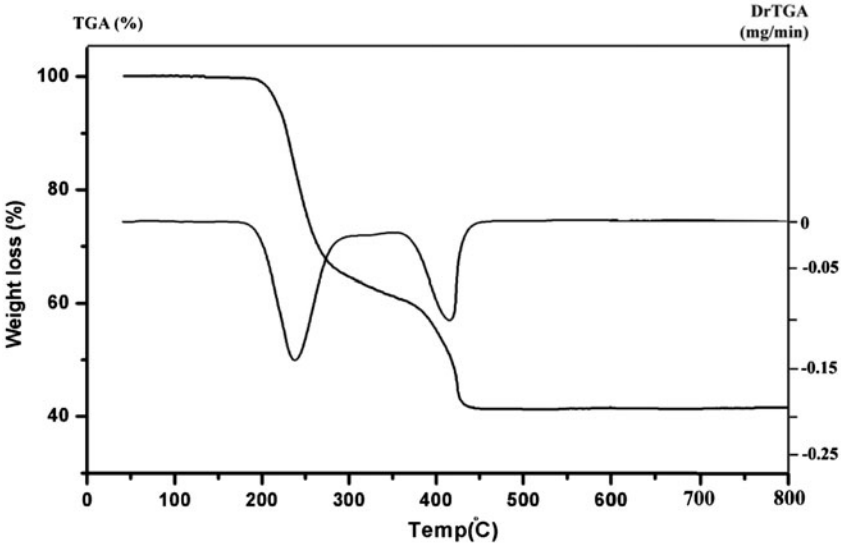

Figure 1. The TG and DTG curves of **1**.

Complex **2** started to decompose at 284 °C with first mass loss at 284–326 °C corresponding to loss of 10.72% of the total weight (calcd 11.48%). This step of decomposition is assigned to the decarboxylation of one bound carboxylate and is accompanied with a DTG peak at 320 °C. The second mass loss of 37.98% is observed at 326–397 °C with a DTG peak at 360 °C; this step is assigned to further decomposition of the ligand yielding the thermally stable Pt residue.

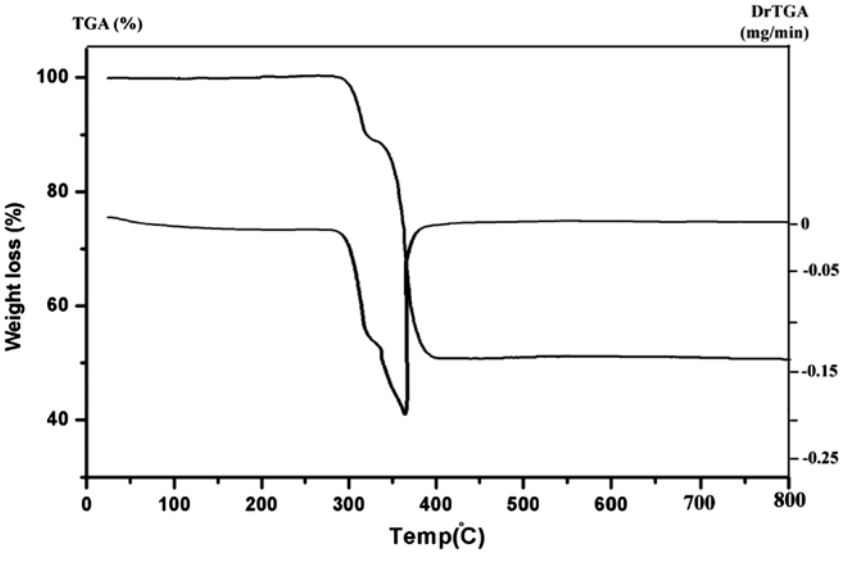

Figure 2. The TG and DTG curves of **2**.

3.3. *Crystal structure of 1*

The molecular structure of **1**, with atom numbering scheme, is shown in figure 3. Selected bond lengths, angles, and hydrogen-bonding geometries are given in tables 2 and 3. Single-crystal X-ray analysis of **1** revealed that it crystallizes in the orthorhombic lattice with *Pnma* space group. The compound possesses a crystallographically imposed mirror symmetry plane along Pt…C4. In the structure of **1**, H_2pdda is neutral bidentate, coordinating to Pt center through the two amino nitrogens. Platinum has cis-$PtCl_2N_2$ coordination. The geometry around Pt is approximately square planar, as expected, with Pt^{2+} coordinating two Cl^- ions and two nitrogens of H_2pdda. The angles around Pt vary from 87.04(7)° to

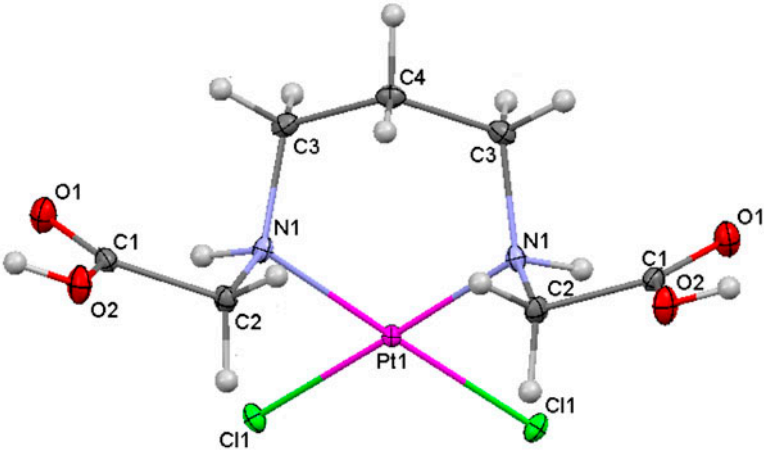

Figure 3. Molecular structure of **1** showing the atom-labeling scheme. Displacement ellipsoids are drawn at the 50% probability level.

Table 2. Selected bond lengths (Å) and angles (°) of **1** and **2a**.

1		**2a**	
Pt1–Cl1	2.3134(7)	Pt1–O1	2.021(3)
Pt1–O3	2.056(2)	Pt1–O3	2.022(3)
O1–C1	1.200(4)	Pt1–N1	2.020(3)
O2–C1	1.334(4)	Pt1–N2	2.022(3)
N1–C3	1.496(4)	O1–C1	1.286(5)
N1–C2	1.481(4)	O2–C1	1.242(5)
C–C1	1.520(4)	N1–C2	1.482(5)
C3–C4	1.514(4)	N2–C5	1.488(4)
O2–H1	0.820(2)	C3–C4	1.521(6)
Cl1 Pt1 N1	177.22(7)	O1 Pt1 O3	95.2(1)
Cl1 Pt1 N1	87.04(7)	O1 Pt1 N1	83.5(1)
Cl1 Pt1 Cl1	92.14(2)	O1 Pt1 N2	178.1(1)
N1 Pt1 N1	93.67(9)	O3 Pt1 N1	178.7(1)
C3 N1 C2	112.5(2)	O3 Pt1 N2	83.5(1
Pt1 N1 C2	114.7(2)	N1 Pt1 N2	97.8(1)
N1 C3 C4	113.5(3)	Pt1 O1 C1	114.0(2)
C3 C4 C3	115.8(3)	Pt1 N1 C2	108.9(2)
N1 C2 C1	110.4(2)	C2 N1 C3	112.0(3)
O1 C1 O2	125.0(3)	Pt1 N2 C6	109.6(2)
O1 C1 C2	124.0(3)	O1 C1 O2	122.1(3)

Table 3. Hydrogen-bond geometry (Å, °) of **1** and **2a**.

D–H···A	D[a]–H	H···A[b]	D···A	D–H···A	Symmetry code at acceptor
Complex **1**					
N1–H1A···O1	0.91	2.38	2.752	104.05	–
O2–H1···Cl1	0.82	2.34	3.169	172.05	$1.5-x, -y, z+0.5$
O2–H1···Cl1	0.82	2.34	3.169	172.05	$1.5-x, y+0.5, z+0.5$
N1–H1A···O2	0.91	2.41	3.18	141.15	$1+x, 0.5-y, z$
N1–H1A···O2	0.91	2.41	3.18	141.15	$1+x, y, z$
Complex **2a**					
N1–H1···O5	0.91	2.05	2.944	166.52	x, y, z
N2–H2···O2	0.91	1.96	2.851	164.76	$x, 1.5-y, 1/2+z$
O3…O6	–	–	2.837	–	$-1+x, y, z$
O5…O6	–	–	2.877	–	x, y, z
O6…O7	–	–	2.956	–	x, y, z
O4…O5	–	–	2.837	–	$1+x, y, z$
O5…O7	–	–	2.844	–	$x, 1.5-y, -1/2+z$
O2…O5	–	–	2.716	–	$x, 1.5-y, -1/2+z$

[a]Acceptor.
[b]Donor.

93.66(13)°. The Pt–Cl distances [2.3134(6) Å] and Pt–N distances [2.056(2) Å] are within the expected values [30]. The chelate ring system, Pt–N1–C3–C4–C3–N1, adopts a chair configuration and the uncoordinated, carboxylates are at axial positions, related across the mirror plane, in the chair form of the six-membered ring.

Crystal packing of the complex is stabilized through strong intra- and inter-molecular hydrogen bonding. One type of intramolecular hydrogen bond is involved, N–H…O. There are many different intermolecular hydrogen bonds in **1** which play an important role in the

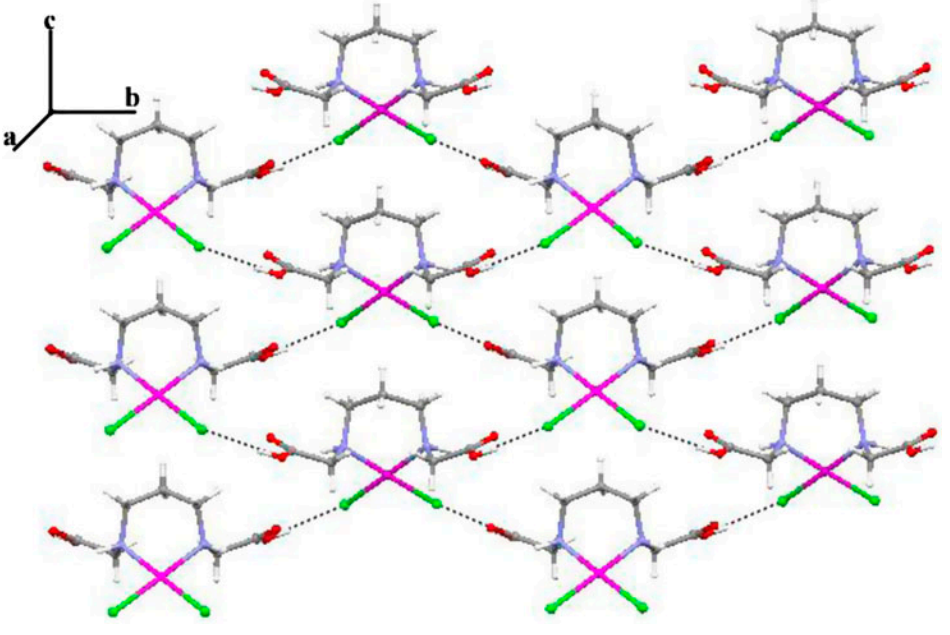

Figure 4. View of the 2-D hydrogen-bonding framework of **1** extended along the *bc* plane.

supramolecular assembly. Molecules are linked through intermolecular O–H…Cl hydrogen bonds, resulting in a 2-D edge-fused motif along the *bc* plane (figure 4). These hydrogen-bonded motifs are linked to form the 3-D network via the N–H…O hydrogen bonds (figure 5).

3.4. *Crystal structure of 2a*

The molecular structure of **2a**, with atom numbering scheme is shown in figure 6. Selected bond lengths, angles, and hydrogen-bonding geometries are given in tables 2 and 3. The complex crystallizes in the monoclinic system with $P2_1/c$ space group. The asymmetric unit is composed of [Pt($C_7H_{12}N_2O_4$)] and three molecules of crystallization water. The deprotonated carboxylates are equatorial with respect to the chair form of this six-membered chelate ring Pt1–N1–C3–C4–C5–N2. The molecular structure revealed a slightly distorted square planar geometry around Pt in which the angles vary from 83.5(1)° to 97.8(1)° (table 2). The value for Pt–O and the Pt–N distances [2.02(3) Å] are similar to the values reported earlier [28, 31]. More than one type of intermolecular hydrogen bond is involved in **2a** and plays a key role in the supramolecular assembly. The most important type is N2–H2…$O2^{i}$ [symmetry code: (i) x, $1.5 - y$, $0.5 + z$] which links molecules resulting in the formation of a 1-D framework (figure 7). The presence of three waters of crystallization gives a 3-D hydrogen-bonded framework which can be represented by figure 8; the O…O distances of crystallization water are listed in table 3.

3.5. In vitro *cytotoxicity*

The antiproliferative effect of **1** and **2** against *liver carcinoma* (HEPG2) and *colon carcinoma* (HCT116) cell lines was conducted in our study and compared with the standard drugs cisplatin (cis-DDP) and Dox. The cytotoxic activities, compared with the two standard drugs, are expressed as IC_{50} which is the concentration required to inhibit 50% of the cell growth when the cells are exposed to the compounds (table 4). In table 4, IC_{50} values

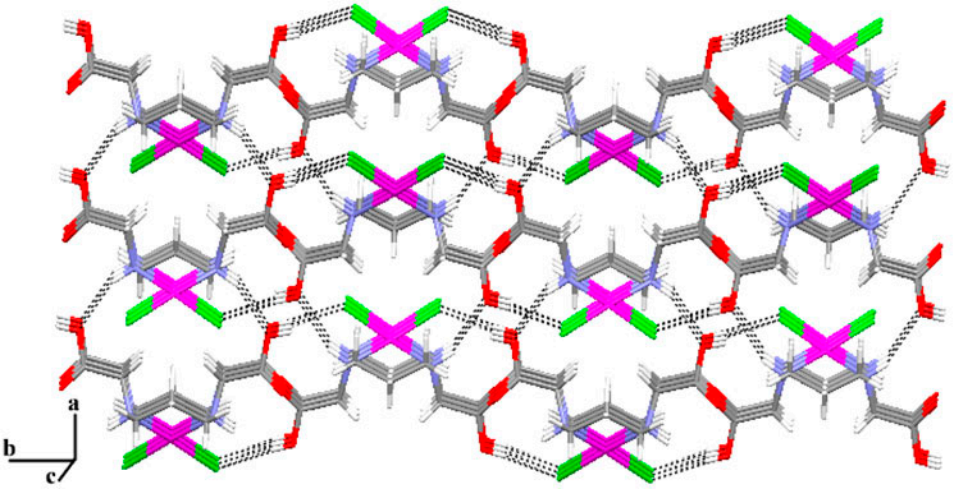

Figure 5. View of the 3-D H-bonded supramolecular framework of **1**.

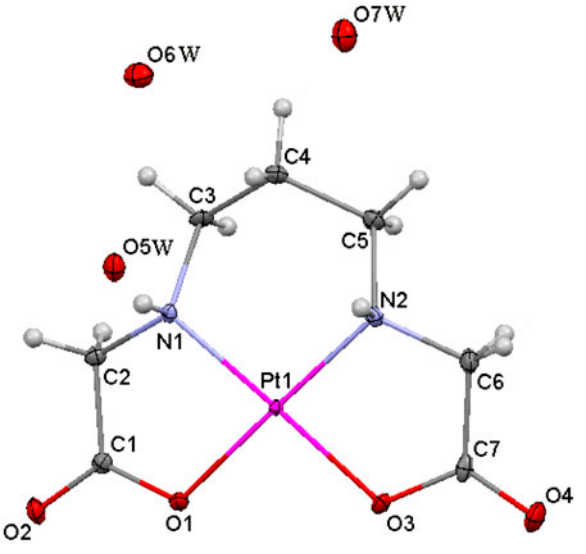

Figure 6. Molecular structure of **2a** showing the atom-labeling scheme. Displacement ellipsoids are drawn at the 50% probability level.

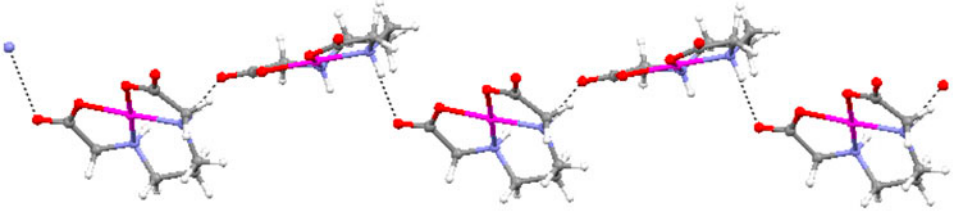

Figure 7. 1-D chain structure of **2a** along the *b*-axis.

are given in μg mL^{-1} and μM. Figures 9 and 10 represent the cytotoxicity of **1** and **2** against the two tested cell lines, using different concentrations of complexes and standard drugs. Untreated cells were used as a control.

The obtained data revealed that **1** and **2** show activity against the two tested cell lines. Each data point is an average of three independent experiments and is expressed as M ± SD. From the obtained data, it is clear that the two complexes inhibit growth of the tested cells in a dose dependent manner. It is also clear that **1** showed an inhibition of cell viability and gave IC_{50} values of 19 and 2.4 μg mL^{-1} against HCT116 and HEPG2, respectively, compared with IC_{50} values of 4.6 and 3.1 against HCT116 and HEPG2, respectively, for cis-DDP and IC_{50} values of 3.2 and 3.1 against HCT116 and HEPG2, respectively, for the standard cytotoxin drug Dox. For **2**, IC_{50} values of 22 and 13.6 μg mL^{-1} against HCT116 and HEPG2, respectively, were obtained. According to Shier [32, 33], compounds with IC_{50} within the range of 10–25 μg mL^{-1} are said to be weak anticancer drugs, those having IC_{50} between 5 and 10 μg mL^{-1} are moderate while compounds of activity below 5.00 μg mL^{-1} are considered strong agents. According to these parameters, **1** and **2** are considered to be

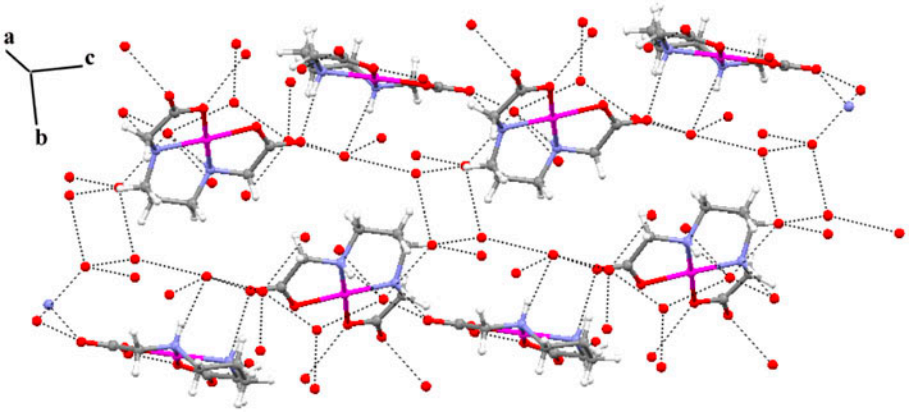

Figure 8. 3-D H-bond structure of **2a**.

Table 4. *In vitro* antitumor activities of **1** and **2** against HCT116 and HEPG2 cell lines.

	IC_{50} μg mL^{-1} (μM)	
Compound	HCT116	HEPG2
1	19 (41.7)	2.4 (5.57)
2	22 (57.4)	13.6 (35.5)
Dox[a]	4.6 (7.9)	3.1 (5.3)
Cis-DDP[b]	3.2 (10.6)	3.1 (10.3)

[a]Doxorubicin.
[b]Standard cytotoxin drug.

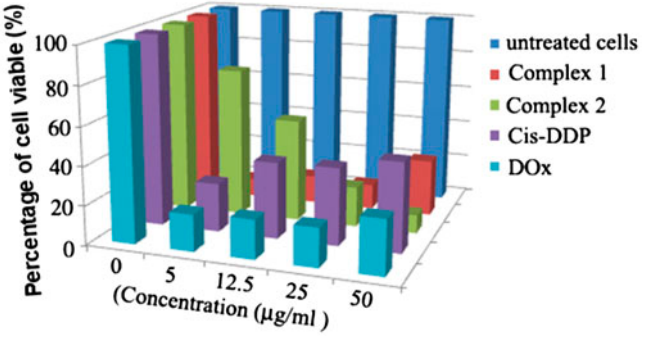

Figure 9. *In vitro* cytotoxicity of **1**, **2**, Dox and cis-DDP against human *liver carcinoma* (HEPG2).

weak anticancer agents against HCT116 and HEPG2, except for **1** which showed strong activity against HEPG2, more cytotoxic than the standard drugs, cis-DDP, and Dox. Structure–activity relationships for platinum coordination compounds confirmed that only those compounds having cis-geometry block tumor cell growth. The most active complex, cisplatin, exhibits antitumor activity, whereas its trans-isomer showed no such activity [34].

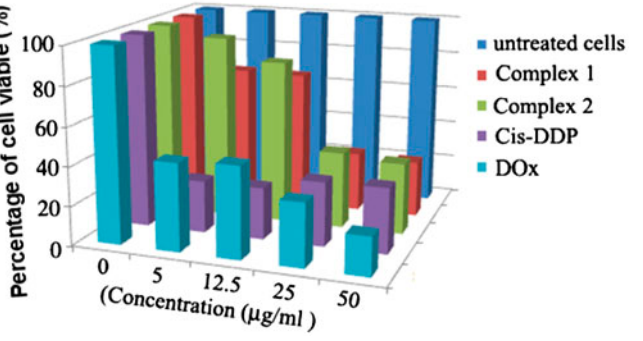

Figure 10. *In vitro* cytotoxicity of **1**, **2**, Dox and cis-DDP against human *colon carcinoma* (HCT116).

Many derivatives of cisplatin also inhibit the growth of tumor cells. The solubility of the complex in water, compared with the insoluble cisplatin, is also a promising goal [35]. The greater bulk of **1**, with its axial carboxylate groups, may play a role in giving it greater activity against HEPG2 compared with cis-DDP. These two factors can explain the relatively high activity of **1**. It is well documented that N-containing ligands, with at least one N–H which is responsible for important hydrogen-bond donor properties, have important effect on cytotoxicity, dependent on the type of the tested cell line [34, 36].

4. Conclusion

Two new Pt(II) complexes of propylenediamine-N,N′-diacetic acid (H_2pdda), [Pt($C_7H_{14}N_2O_4$)Cl_2] (**1**), and [Pt($C_7H_{14}N_2O_4$)] (**2**) have been synthesized and characterized. The obtained data indicate that H_2pdda is bidentate and tetradentate for **1** and **2**, respectively. The crystal structure of **1** and [Pt($C_7H_{12}N_2O_4$)]·3H_2O (**2a**) indicate that the two compounds formed 3-D hydrogen-bonded frameworks. The *in vitro* cytotoxic properties of **1** and **2** were evaluated against HEPG2 and HCT116 and compared with two standard anticancer drugs, cis-platin (cis-DDP) and Dox. The obtained data reveal that the two complexes showed poor cytotoxic activity against HEPG2 and HCT116 except for **1** which exhibited high activity against HEPG2, even more than the standard drugs. The cis-geometry of **1**, which is correlated with the structure of cisplatin, may be the key factor for such reactivity. The N-containing ligand and the high solubility of **1** and **2** also have important effects on cytotoxicity. Consequently, the cytotoxicity of **1** and **2** deserves further study.

Supplementary material

CCDC 917388 and 917389 contain the supplementary crystallographic data for **1** and **2a**, respectively. These data can be obtained free of charge via http://www.ccdc.cam.ac.uk/conts/retrieving.html or from the Cambridge Crystallographic Data Center, 12 Union Road, Cambridge CB2 1EZ, UK; Fax: +44 1223336033; or E-mail: deposit@ccdc.cam.ac.uk.

References

[1] B. Rosenberg, L. van Camp, T. Krigas. *Nature*, **205**, 698 (1965).
[2] T. Boulikas, M. Vougiouka. *Oncol. Rep.*, **10**, 1663 (2003).
[3] C.A. Rabik, M.E. Dolan. *Cancer Treat. Rev.*, **33**, 9 (2007).
[4] N. Summa, T. Soldatovic, L. Danlenburg, Z.D. Bugarcic, R.V. Eldik. *J. Biol. Inorg. Chem.*, **12**, 461 (2007).
[5] H. Silva, C.V. Barra, F.V. Rocha, F. Frézard, M.T.P. Lopesc, A.P.S. Fontes. *J. Braz. Chem. Soc.*, **21**, 1961 (2010).
[6] G. Daugaard, U. Abildgaard. *Cancer Chemother. Pharmacol.*, **25**, 1 (1989).
[7] D. Screnci, M.J. McKeage. *J. Inorg. Biochem.*, **77**, 105 (1999).
[8] L. Galluzzi, L. Senovilla, I. Vitale, J. Michels, I. Martins, O. Kepp, M. Castedo, G. Kroemer. *Oncogene*, **31**, 1869 (2012).
[9] A.P.S. Fontes, S.G. de Almeida, L.A. Nader. *Quim. Nova*, **20**, 398 (1997).
[10] R. Zaludova, A. Zakovska, J. Kasparkova. *Eur. J. Biochem.*, **246**, 508 (1997).
[11] I. Kostova. *Recent Patents Anti-Cancer Drug Discovery*, **1**, 1 (2006).
[12] K. Ota. *Jpn. J. Cancer Chemother.*, **23**, 379 (1996).
[13] R.B. Weiss, M.C. Christian. *Drugs*, **46**, 360 (1993).
[14] L.R. Kelland, M.J. McKeage. *Drugs Aging*, **5**, 85 (1994).
[15] P.J. Bednarski, F.S. Mackay, P.J. Sadler. *Anti-Cancer Agents Med. Chem.*, **7**, 75 (2007).
[16] D.H. Busch, J.C. Bailar. *J. Am. Chem. Soc.*, **78**, 716 (1956).
[17] C.F. Liu. *Inorg. Chem.*, **3**, 680 (1964).
[18] B.B. Smith, D.T. Sawyer. *Inorg. Chem.*, **8**, 1154 (1969).
[19] N.N. Zhdigovoskaya, C.R. Shchelokova, L.V. Popov, V.I. Spytsin. *Koord. Khim.*, **10**, 107 (1984).
[20] R.E. Shepherd, S. Zhang, R. Kortes, F.T. Lin, C. Maricondl. *Inorg. Chim. Acta*, **244**, 15 (1996).
[21] J.T. Whalen, S.-C. Chang, R.E. Norman. *Acta Crystallogr.*, **52C**, 297 (1996).
[22] M. Mullaney, S. Chang, R.E. Norman. *Inorg. Chim. Acta*, **265**, 275 (1997).
[23] Bruker APEX2. Bruker AXS Inc., Madison, Wisconsin, USA (2006).
[24] G.M. Sheldrick. *SADABS*, University of Gottingen, Germany (1996).
[25] G.M. Sheldrick. *Acta Crystallogr.*, **64A**, 112 (2008).
[26] K. Sakai. *KENX*, Kyushu University, Japan (2004).
[27] P. Skehan, R. Storeng. *J. Natl. Cancer Inst.*, **82**, 1107 (1990).
[28] V.M. Dinovic, G.A. Bogdanovic, S. Novakovic, T.J. Sabo. *J. Coord. Chem.*, **57**, 535 (2004) (and references therein).
[29] K. Nakamoto. *Infrared Spectra of Inorganic and Coordination Compound*, Wiley, New York, NY (1986).
[30] J. Zhang, Q. Liu, C. Duan, Y. Shao, J. Ding, J. Miao, X. You, Z. Guo. *J. Chem. Soc., Dalton Trans.*, 591 (2002).
[31] G.N. Kaluderovic, G.A. Bogdanovic, T.J. Sabo. *J. Coord. Chem.*, **55**, 817 (2002).
[32] W.T. Shier. *Mammalian Cell Culture on $5 a Day: A Lab Manual of Low Cost Methods*, University of the Philippines, Los Banos (1991).
[33] N.T. Abdel-Ghani, A.M. Mansour. *J. Coord. Chem.*, **65**, 763 (2012).
[34] I. Kostov. *Recent Patents Anti-Cancer Drug Discovery*, **1**, 1 (2006).
[35] J. Zhang, Y. Gong, X. Zheng. *Synth. React. Inorg. Met.-Org. Chem*, **32**, 49 (2002).
[36] J. Zhang, L. Ma, F. Zhang, Z. Zhang, L. Li, S. Wang. *J. Coord. Chem.*, **65**, 239 (2012).